

See discussions, stats, and author profiles for this publication at: <https://www.researchgate.net/publication/51680435>

Photophysics of Untethered ZnTPP–Fullerene Complexes in Solution

ARTICLE *in* THE JOURNAL OF PHYSICAL CHEMISTRY A · SEPTEMBER 2011

Impact Factor: 2.69 · DOI: 10.1021/jp2082853 · Source: PubMed

CITATIONS

14

READS

156

7 AUTHORS, INCLUDING:



Sunish K Sugunan

Mahatma Gandhi University

5 PUBLICATIONS 62 CITATIONS

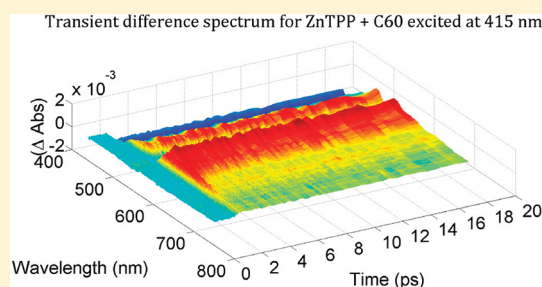
SEE PROFILE

Photophysics of Untethered ZnTPP–Fullerene Complexes in Solution

Sunish K. Sugunan,[†] Benjamin Robotham,[‡] Ryan P. Sloan,[†] Jędrzej Szmytkowski,^{†,§} Kenneth P. Ghiggino,^{*,†} Matthew F. Paige,^{*,†} and Ronald P. Steer^{*,†}[†]Department of Chemistry, University of Saskatchewan, 110 Science Place Saskatoon, SK, Canada S7N 5C9[‡]School of Chemistry, University of Melbourne, Parkville, Victoria 3010, Australia

S Supporting Information

ABSTRACT: The spectroscopy and dynamic behavior of the self-assembled, Soret-excited zinc tetraphenylporphyrin (ZnTPP) plus fullerene (C₆₀) model system in solution has been examined using steady state fluorescence quenching, nanosecond time-correlated single photon counting, picosecond fluorescence upconversion, and picosecond transient absorption methods. Evidence of ground state complexation is presented. Steady-state quenching of the S₂ and S₁ fluorescence of ZnTPP by C₆₀ reveals that the quenching processes only occur in the excited complexes, are ultrafast, and proceed at different rates in the two states. Only uncomplexed ZnTPP is observed by fluorescence lifetime methods; the locally excited complexes are either dark or, more likely, rapidly relax to products that do not radiate strongly. Both short-range (Dexter) energy transfer and electron transfer relaxation mechanisms are evaluated. Picosecond transient absorption data obtained from the subtle differences between the spectra of Soret-excited ZnTPP with and without a large excess of added C₆₀ reveal the formation, on a subpicosecond time scale, of relatively long-lived charge-separated species. Soret excitation of ZnTPP ··· C₆₀ does not produce a quantitative yield of species in the lower S₁ excited state.



INTRODUCTION

Articles now numbered in the thousands describe a multitude of opportunities for utilizing the unusual spectroscopic and photophysical properties of the porphyrins and the fullerenes, both separately and together, in constructing useful photon-actuated devices.¹ Prominent among these are studies of the spectroscopic and photophysical properties of porphyrin–fullerene dyads, triads and other supramolecular constructs used to produce long-lived, charge-separated species of critical importance in the successful operation of optoelectronic switches, devices for artificial photosynthesis and organic solar photovoltaic cells.²

In our studies of the potential for using noncoherent photon upconversion (NCPU) via triplet–triplet annihilation (TTA) to improve the overall efficiency of solar photovoltaic cells, we have undertaken to generate fundamental photophysical data on model metalloporphyrins (zinc and tin tetraphenylporphyrins, ZnTPP and SnTPPCL₂),³ with and without noncovalently bound ligands (pyridine, pyrazine, bipyridine)⁴ and fullerenes (C₆₀ and C₇₀) in a variety of media.⁵ Our approach has been different from those taken by others in the field who have effected upconversion by employing energy transfer from the triplet of the absorber to the triplet state of a second component in which TTA occurs to produce its lowest excited (upconverted) singlet state.⁶ We have concentrated on systems, such as the porphyrins⁷ (and thiones⁸ and azulenes⁹) in which the absorber and upconverter are one in the same species, and in which upconversion occurs by homomolecular TTA to produce an upper electronically excited singlet state that can act as a potential electron donor in a photovoltaic

cell. That is, we wish to exploit the sequence: $MP(S_0) + h\nu_{NIR} \rightarrow MP(S_1) \rightarrow MP(T_1)$; $2MP(T_1) \rightarrow MP(S_2) + MP(S_0)$; $MP(S_2) + A \rightarrow MP^{*+} + A^{*-}$, where MP is the metalloporphyrin and A is a suitable electron acceptor. To our surprise, we have found little relevant information on the photophysics of the shorter-lived excited singlet states of these porphyrins in the presence of unsubstituted, untethered fullerenes, which are often electron acceptors of choice. In particular, there is no information at all on the fs to ps dynamics of the untethered ZnTPP ··· C₆₀ model system excited at wavelengths in the porphyrin Soret band region.

One of the most important aspects of utilizing metalloporphyrins as dual absorber-upconverters is the fate of the initially formed upconverted S₂ state in the presence of potential electron and/or energy acceptors. Clearly, if the MP(S₂) states are to serve as the electron donors in photovoltaic cells or other devices, the donor–acceptor electron transfer and charge separation processes must be considerably faster than the rates of other parallel intramolecular and intermolecular decay processes of the excited molecule. Inasmuch as the longest-lived MP(S₂) states have lifetimes that are only a few ps under normal conditions,³ this is a tall order. Nevertheless, electron transfer rates of porphyrin S₂ states approaching 10¹³ s^{−1} have been measured,¹⁰ and offer promise of being competitive with energy-wasting intramolecular relaxation processes.

Received: August 26, 2011

Revised: September 28, 2011

Published: September 29, 2011

Previous reports of the photophysics of self-aggregating MP–fullerene systems in solution have focused on the kinetics of energy and electron transfer between the triplet states of the MP and the fullerene.^{1b} Thus Ito and co-workers¹¹ using ns transient absorption methods determined that excitation of rather concentrated solutions of ZnTPP in benzonitrile resulted in electron transfer rates from the porphyrin triplet to the C₆₀ and C₇₀ fullerenes in the $(5-7) \times 10^8 \text{ M}^{-1} \text{ s}^{-1}$ range whereas excitation of the fullerene resulted in the ground state of the ZnTPP transferring an electron to the fullerene triplet with rate constants in the $(8-10) \times 10^8 \text{ M}^{-1} \text{ s}^{-1}$ range.

When the porphyrin is excited in the Soret region, however, the dynamics can be altogether different. Depending on the electronic energies and the reduction potential of the putative electron acceptor, the nature and properties of the surrounding medium and the ground state interaction energy between the porphyrin and the addend, decay of the initially excited S₂ state of the porphyrin could occur either by electronic energy transfer or by electron transfer. Both have been reported in studies of the relaxation processes of Soret excited porphyrins in covalently tethered dyads and larger supramolecular constructs. Thus Mataga and co-workers¹⁰ propose that the S₂ states of Soret-excited, directly covalently bound porphyrin–imide dyads relax almost exclusively by electron transfer from the metalloporphyrin donor to the imide acceptor. In these cases, energy transfer from the S₂-excited porphyrin to the imide is endergonic and the perpendicular imide moiety, although directly bonded to the porphyrin, is only weakly electronically coupled to it. Mataga et al. map out the full normal, barrierless and inverted Marcus regions of electron transfer from the Soret excited moiety by varying the reduction potentials of the imide acceptor groups, and find that very rapid electron transfer rates of up to $7 \times 10^{12} \text{ s}^{-1}$ occur in the barrierless region.

On the other hand when the putative electron acceptor has electronic states that lie lower than that of the Soret-excited porphyrin, both energy and electron transfer are possible. Thus, Kesti et al.¹² report that the S₂ states of Soret-excited covalently linked porphyrin–C₆₀ or –C₇₀ dyads relax primarily by S₂–S₁ internal conversion within the excited porphyrin moiety and by parallel intramolecular energy transfer to the fullerene. They conclude that electron transfer from the porphyrin in its locally excited S₂ state to the fullerene is only a remote possibility in the C₇₀ dyad. Reports of the photophysics of larger porphyrin–fullerene constructs are legion,^{1,2} but little definitive information is available about the fate of the initial locally excited Soret state. Indeed, it is sometimes presumed¹³ that excitation of a porphyrin–fullerene dyad in the Soret region will populate the S₁ local excited state of the porphyrin quantitatively within the normal ps intramolecular radiationless decay time of the initially excited S₂ state.

Curiously, there are no reports of the ultrafast dynamics of self-aggregated, untethered metalloporphyrin–fullerene systems excited in the porphyrin Soret bands in solution. As discussed by Mataga et al.,^{10a} such an investigation will be burdened by the intrinsic difficulty of interpreting quenching of the excited porphyrin when the interactions between it and the fullerene are weak and characterized by a distribution of intermolecular distances. Nevertheless, such an investigation can be expected to provide insight into intermolecular interactions in more structurally complex aggregated systems found in devices, when subjected to Soret excitation.

In this article we describe the spectroscopy and photophysics of self-aggregated ZnTPP–C₆₀ complexes in arene solutions,

excited throughout the near UV–visible spectrum, and compare the results with those from larger tethered and substituted fullerene–porphyrin pairs and supramolecular systems.

EXPERIMENTAL SECTION

ZnTPP (low chlorin), C₆₀ (99.9% purity), toluene (HPLC grade, $\geq 99.9\%$ purity), and benzonitrile were purchased from Sigma-Aldrich and were used as received. Whenever possible, low ZnTPP concentration solutions were employed to avoid self-aggregation of the porphyrin. Toluene does not form charge transfer complexes with C₆₀,¹⁴ and most measurements were made in aerated toluene solutions at room temperature.

Absorption spectra were taken using the short path of a $1 \times 10 \text{ mm}$ or a $2 \times 10 \text{ mm}$ optical cell with a Varian-Cary 500 spectrophotometer. Steady state fluorescence measurements were measured using a PTI Quantamaster spectrofluorimeter. Samples were excited through the long path and the fluorescence emission was measured through the short path of a $2 \times 10 \text{ mm}$ cuvette to minimize the effect of fluorescence reabsorption, which is particularly severe in the porphyrin Soret region. Artifacts in the emission spectra due to solvent Raman scattering and fluorescence reabsorption by both ZnTPP and C₆₀ were corrected using procedures described in detail previously.¹⁵ Additional normalization corrections to account for the attenuation of light at the fluorescence excitation wavelength by added C₆₀ are outlined in the Supporting Information.

Nanosecond S₁ fluorescence decays were measured using a time-correlated single-photon counting (TCSPC) setup which is described in detail elsewhere.¹⁶ Samples were excited at 407 nm through the long path and the 650 nm fluorescence emission was measured at the magic angle through the short path of a $2 \times 10 \text{ mm}$ cuvette. A long pass filter was used on the emission monochromator side to filter the 407 nm excitation laser scattering whenever necessary. A complex weak emission decay from C₆₀ solutions alone, which could not be fitted well using even a four exponential model and which extended beyond the usual 50 ns data acquisition time window was subtracted, after IRF deconvolution, from the experimental decay data to get the true ZnTPP fluorescence decay curves for the ZnTPP–C₆₀ mixtures. Fortunately this weak component constituted less than 2% of the total emission from the mixtures even at C₆₀:ZnTPP molar ratios of 1000:1 and therefore had no significant effect on the accuracy of the measurement of the decay characteristics of the main S₁ ZnTPP emission at 650 nm.

Picosecond ZnTPP S₂ temporal fluorescence decay profiles and S₁ rise time profiles were measured using femtosecond fluorescence upconversion instrumentation, as described in detail earlier.^{3b,c} Samples of 180 μM porphyrin concentration were excited at 400 nm, S₂ fluorescence decays were measured at 433 nm and the S₁ fluorescence rise profiles were measured at 655 nm. These emission profiles showed no evidence of additional ps fluorescence decay or rise components due to C₆₀ itself even though absorption of a significant fraction of the 400 nm excitation by C₆₀ is unavoidable. Carrying out the experiments in aerated solutions suppressed delayed S₂ fluorescence due to triplet–triplet annihilation.

Picosecond transient absorption spectra were recorded using an ultrafast excitation source consisting of a Ti:sapphire laser (Coherent, Mira) combined with a regenerative amplifier (Coherent, RegA 9050) operating at a 94 kHz pulse repetition rate and with an average output power of $\sim 500 \text{ mW}$ at 830 nm.

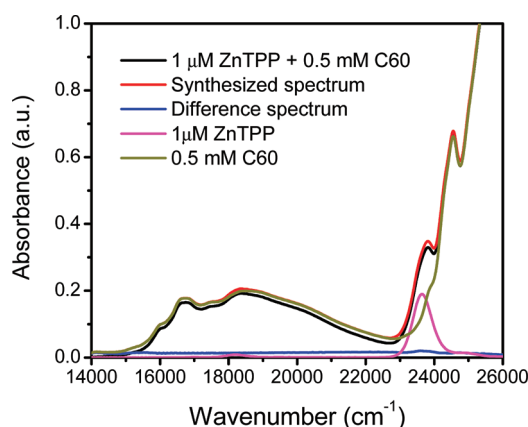


Figure 1. Normalized absorption spectra of (i) 1 μM ZnTPP, (ii) 0.5 mM C_{60} , (iii) a mixture of 1 μM ZnTPP + 0.5 mM C_{60} , (iv) a synthesized spectrum of (i) + (ii), and (v) the difference between (iii) and (iv), all in toluene at room temperature. The spectral bandpass is 2.0 nm. Spectrum iv is displaced by 0.01 au relative to spectrum iii, and spectrum v is displaced relative to spectrum i for clarity of comparison.

Half of the amplified output was directed to an OPA (Coherent, OPA 9400) and the second harmonic output at 415 nm was used as the pump beam with an average power of ~ 70 mW. This pump beam was modulated with a light chopper (Thorlabs, MC1000/MC1F60) before passing through a variable optical delay line (Newport, UTS150PP with ESP 300 controller) and a Berek compensator (New Focus, 5540) to the sample cell (Starna, 2 mm path length). The other half of the amplified laser output was focused into a 3 mm sapphire crystal (Crystalsystems) to provide a continuum probe beam with an employed range of 460 to 760 nm.

The relative polarization of the pump and probe beams are set to 54.7 degrees (the magic angle) to remove any distortion effects due to molecular rotation. After passing through the sample the probe beam is delivered to a CMOS detector (Ultrafast Systems) by a 200 μm fiber (Ocean Optics, P200-2-UV-vis). Data acquisition was controlled by a MATLAB (Mathworks) program developed in-house. All spectra were corrected for the chirp of the probe continuum. The time resolution of the system is approximately 200 fs.

Samples of ZnTPP (100 μM in both toluene and benzonitrile), C_{60} (1 mM in toluene, 0.2 mM in benzonitrile) and a mixture of both with identical respective concentrations were excited with 415 nm pulses and probed as described above in the 460 to 760 nm region. An interval of 20 ps was scanned with 200 logarithmically spaced delay positions and the spectra collected were averaged over 20 scans. All measurements were carried out in aerated solutions to minimize the build-up of long-lived triplet species. The solutions in the sample cell were stirred continuously during measurement by a magnetic stirrer bead.

RESULTS

The UV-visible absorption spectra of ZnTPP, of C_{60} and of a typical ZnTPP- C_{60} mixture, all in aerated toluene at room temperature, are shown in Figure 1. The spectra of ZnTPP and of C_{60} separately are identical in all respects to previously published solution spectra taken under similar conditions.^{1,3} As previously observed,^{12,17} the UV-visible spectra of the mixtures at C_{60} :ZnTPP molar ratios up to at least 1000:1 and at ZnTPP concentrations low enough to avoid significant aggregation are

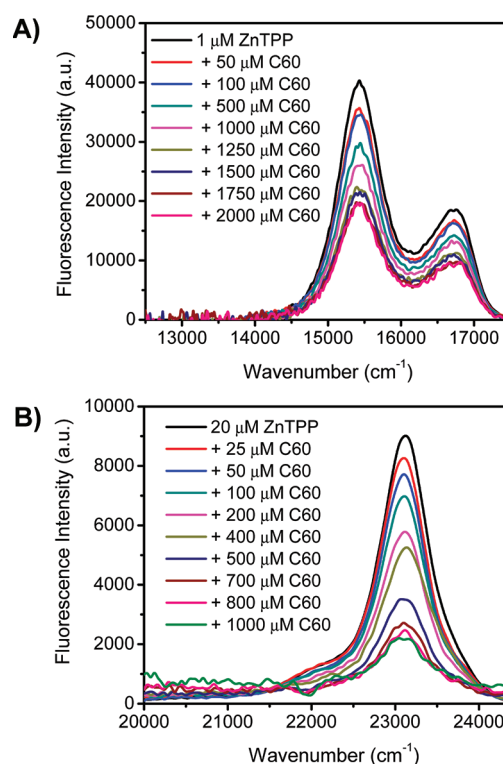


Figure 2. (A) S_1 fluorescence quenching of 1.0 μM ZnTPP upon addition of increasing concentrations of C_{60} when excited at 550 nm. Excitation and emission band passes were fixed at 2.0 and 4.0 nm, respectively. See text for spectral correction procedures. (B) S_2 fluorescence quenching of 20.0 μM ZnTPP upon addition of increasing concentrations of C_{60} when excited at 400 nm. Both excitation and emission band passes were fixed at 2.0 nm. See text for spectral correction procedures.

identical to the synthetic spectra obtained by digitally summing the spectra of the individual components at the same concentration. The difference spectrum is also shown in Figure 1. At the resolution and concentrations employed, the bands in the spectra of the mixtures show no evidence of significant broadening or shift and no new band appears. The weak charge transfer band seen in solid state and thin film metalloporphyrin-fullerene assemblies¹⁸ is not observed at these concentrations. Allowing for minor statistical concentration uncertainties and measurement errors, the difference spectrum reproduces the instrument baseline.

These results are contrary to a recent report¹⁹ in which the association constants of zinc tetrahexylporphyrin with C_{60} and C_{70} in toluene were determined by following an apparent decrease in the peak absorbance of the Soret band with added fullerene. We find that when the spectrophotometer's spectral bandwidth and data acquisition step size are sufficiently small there is no statistically significant change in the integrated absorbance of either the Soret or the Q-band for up to a 1000-fold excess of C_{60} :ZnTPP (cf. detail in the Supporting Information).

Quenching of both S_1 and S_2 fluorescence of ZnTPP is observed when C_{60} is added to the solution, as shown in the steady state spectra, Figure 2A,B. These spectra are corrected for increasing competitive absorption by C_{60} at the excitation wavelength, for reabsorption by both ZnTPP and C_{60} and for background scatter (which itself is corrected for competitive

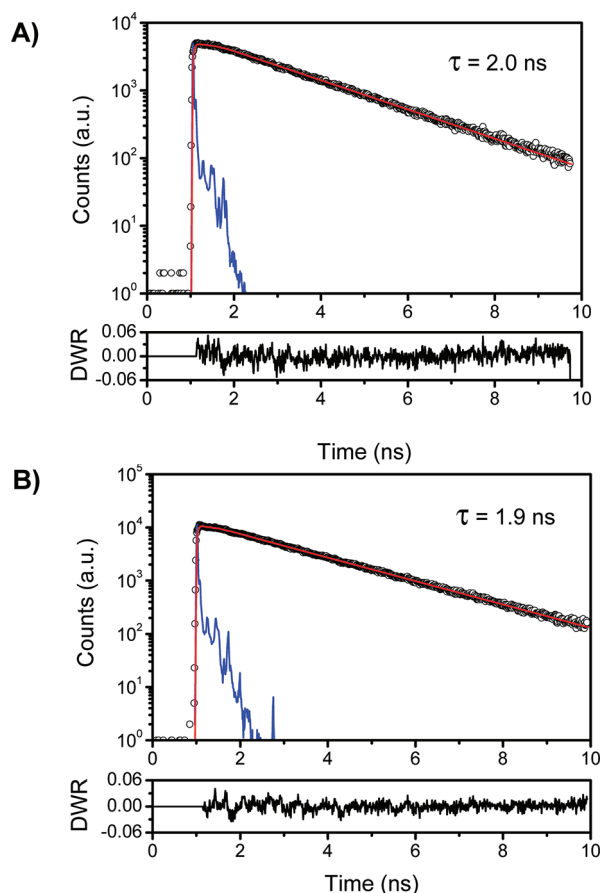


Figure 3. (A) S_1 – S_0 fluorescence decay of $1.0\ \mu\text{M}$ ZnTPP, excited at $407.0\ \text{nm}$ and monitored at $650.0\ \text{nm}$. Open circles are the data points ($9.7\ \text{ps}$ per channel), and the solid blue line is the instrument response function. The solid red line is the best single exponential fit to the data determined by the reduced χ^2 value. The lower panel shows the distribution of the weighted residuals. (B) S_1 – S_0 fluorescence decay of $1.0\ \mu\text{M}$ ZnTPP with $1.0\ \text{mM}$ added C_{60} excited at $407.0\ \text{nm}$ and monitored at $650.0\ \text{nm}$. The solid line is the best single exponential fit to the data determined by the reduced χ^2 value. The lower panel shows the distribution of the weighted residuals. Data were obtained at $9.7\ \text{ps}$ /channel.

absorption by C_{60} at the excitation wavelength). The raw spectra exhibit significant emission in the $15000\ \text{cm}^{-1}$ to $12000\ \text{cm}^{-1}$ region due to the excitation of C_{60} itself, and this is digitally subtracted in the spectra shown in these figures. At the low ZnTPP concentrations employed (to avoid their aggregation) no significant additional emission from either C_{60} or a charge transfer complex between ZnTPP and C_{60} could be detected at high C_{60} :ZnTPP ratios when exciting in either the porphyrin Q or Soret bands.

Note that S_2 fluorescence of the porphyrin is quenched considerably more efficiently than that of S_1 emission for the same relative concentrations of C_{60} :ZnTPP, despite the fact that the lifetime of the S_2 state is about 3 orders of magnitude shorter than that of S_1 . A comparison of the corrected S_1 – S_0 steady state emission spectra obtained by exciting in the Soret and Q bands (not shown; cf. Section 3 in the Supporting Information) shows that the shapes and relative intensities of the emission bands are identical. However the relative intensity of the quenched S_1 (Q-band) fluorescence is lower per unit absorbance

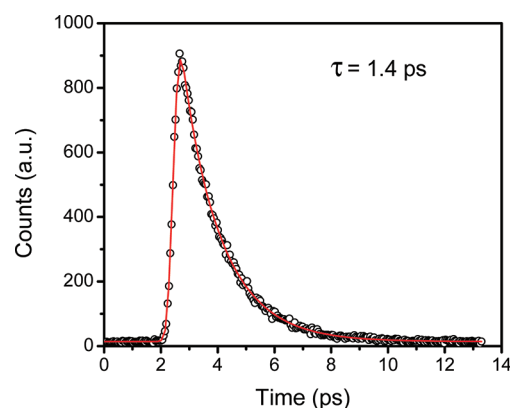


Figure 4. Temporal S_2 fluorescence decay of $180\ \mu\text{M}$ ZnTPP with $900\ \mu\text{M}$ added C_{60} in toluene excited at $400\ \text{nm}$ and monitored at $433\ \text{nm}$. The red curve shows the best single exponential fit to the data, with $\tau = 1.40\ \text{ps}$. The data are obtained at $46\ \text{fs}$ per point.

and per unit concentration of added C_{60} when exciting in the Soret band compared with the Q-band. This can be ascribed to the competitive quenching of the S_2 state by C_{60} on a subps time scale, which lowers the quantum yield of S_1 formed via S_2 – S_1 internal conversion in the initially Soret-excited ZnTPP fluorophore of the ZnTPP $\cdots \text{C}_{60}$ complex (vide infra).

All of the above steady state experiments were also carried out in benzonitrile, a solvent chosen for its ability to stabilize possible charge transfer products of the interaction between excited ZnTPP and added C_{60} . The results are qualitatively similar to those obtained in toluene, but the lower solubility of C_{60} in the polar solvent limited the range of concentrations that could be investigated. Data of poorer quality were obtained; nevertheless, these data indicate that no significant difference in the photo-physics is observed in the polar solvent compared with toluene. No direct evidence in favor of photon-initiated electron transfer and stabilization of ion pair products was found, however.

Parts A and B of Figure 3 illustrate that adding large excesses of C_{60} have no significant effect on the measured ns temporal fluorescence decay profiles in the Q-band region. The observed decays are corrected by subtracting the small amount of background due to C_{60} alone. After this correction, the fluorescence profiles are well-represented by the same single exponential decay function with a lifetime of $2.00 \pm 0.05\ \text{ns}$ at all C_{60} concentrations up to ca. $2\ \text{mM}$. At these highest C_{60} concentrations (a 2000:1 excess) more than half of the ZnTPP will be complexed with C_{60} in the ground state (vide infra) and the steady state fluorescence intensity has decreased by about a factor of 2 (cf. Figure 2A). This fluorescence lifetime is characteristic of an unquenched, unperturbed S_1 state of ZnTPP in aerated toluene.²⁰ A very minor shorter-lived decay component ($<2\%$ of the total emission at all C_{60} concentrations up to $1\ \text{mM}$) is detected at this emission wavelength and apparently increases in amplitude at much higher C_{60} concentrations (see data in section 4 of the Supporting Information). However, at these highest concentrations subtraction of the C_{60} component results in very noisy, imprecise data to which we are reluctant to ascribe much significance.

Figure 4 shows the apparently negligible effect of adding a large excess of C_{60} on the ps temporal fluorescence profile of the S_2 state of ZnTPP in toluene. Again, although the steady state S_2 fluorescence intensity is significantly lower at the higher C_{60} concentrations used in these experiments, the observed

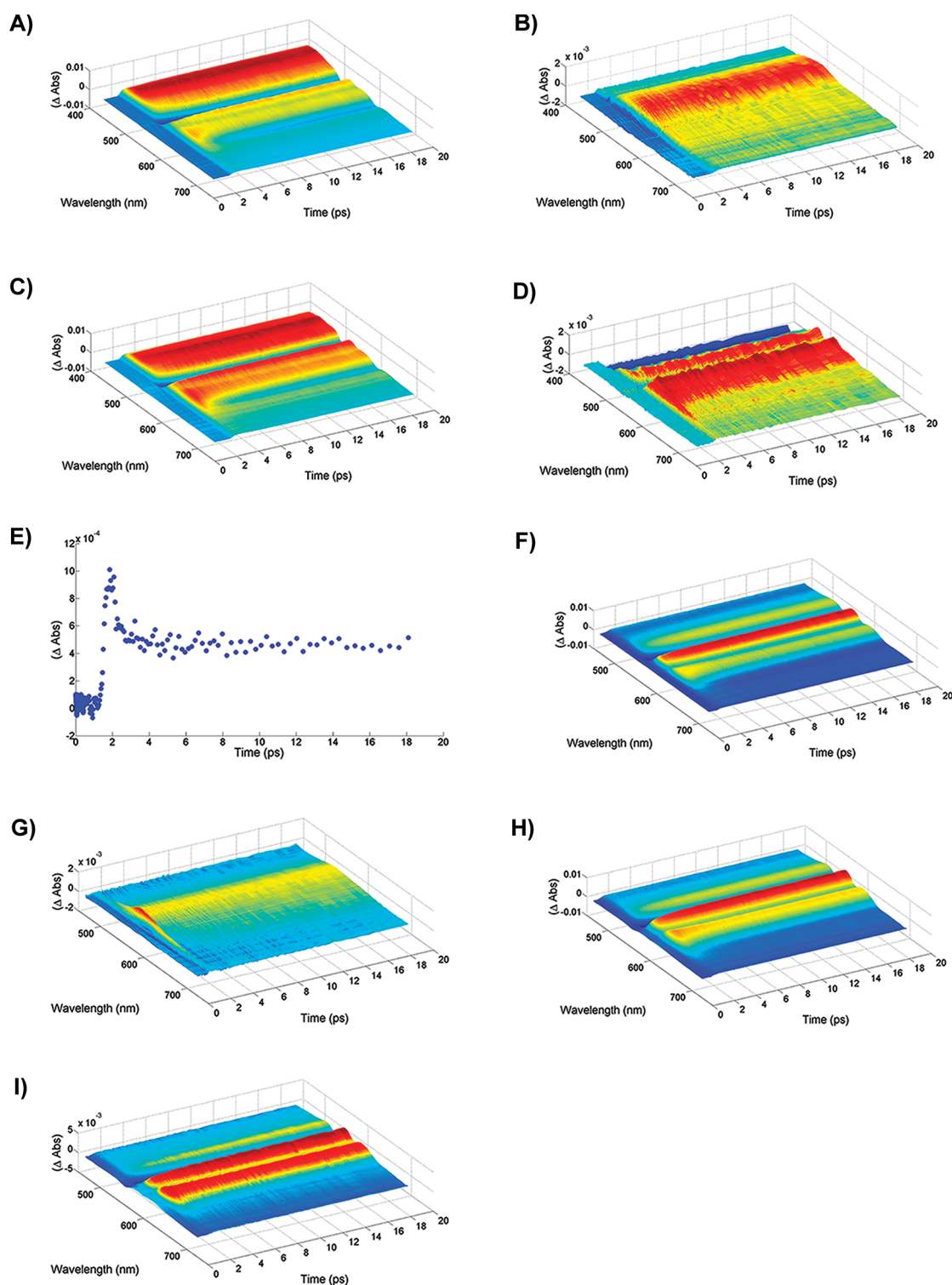


Figure 5. (A) Transient absorption spectrum of 100 μM ZnTPP in toluene excited at 415 nm. (B) Transient absorption spectrum of 1 mM C_{60} in toluene excited at 415 nm. (C) Transient absorption spectrum of 100 μM ZnTPP with 1 mM added C_{60} in toluene excited at 415 nm. (D) Absorbance adjusted difference spectrum of (C) (ZnTPP + C_{60}) – (A) (ZnTPP) – (B) (C_{60}) in toluene. (E) Kinetic trace of the absorbance adjusted difference spectrum (D) at 650 nm. (F) Transient absorption spectra of 100 μM ZnTPP in benzonitrile excited at 415 nm. (G) Transient absorption spectra of 200 μM C_{60} in benzonitrile excited at 415 nm. (H) Transient absorption spectra of 100 μM ZnTPP with 200 μM added C_{60} in benzonitrile excited at 415 nm. (I) Absorbance adjusted difference spectrum of (H) (ZnTPP + C_{60}) – (F) (ZnTPP) – (G) (C_{60}) in benzonitrile.

fluorescence decay profile remains monoexponential and the lifetime remains unchanged at 1.40 ± 0.05 ps, a value characteristic of an unperturbed, unquenched S_2 excited state of uncomplexed

ZnTPP in toluene.^{3a} The S_1 fluorescence rise profiles (not shown; cf. section 5 of the Supporting Information), although much noisier due to the smaller oscillator strength of the S_1 – S_0 transition, also

exhibit no significant change in their temporal behavior; the rise time remains equal (within ca. ± 0.1 ps) to the S_2 fluorescence decay time of unquenched ZnTPP at all added C_{60} concentrations.

The transient absorption spectrum of ZnTPP in toluene in Figure 5A is dominated by the strong absorption bands around 470, 575, 610, and 676 nm previously attributed^{10,21} to the S_1 state. The weaker feature with a maximum around 650 nm exhibits the same decay rate as does the fluorescence in Figure 4, is novel, and is assigned to absorption by the S_2 state of ZnTPP itself. The transient absorption spectrum of C_{60} in toluene in Figure 5B shows the long-lived, very broad absorption with minor maxima at 544 and 648 nm clearly assignable to its S_1 state.

The transient absorption spectrum of the ZnTPP + C_{60} mixture in toluene shown in Figure 5C is very similar to that of ZnTPP without C_{60} present. However, the band at blue end of the detection range is significantly reduced in amplitude while the amplitude in the region above 500 nm, especially around 650 nm, is markedly increased. To further quantify this observation the relative absorbance-corrected transient spectra of ZnTPP and C_{60} were subtracted from the spectrum of the mixture as shown in Figure 5D. Because the absorbance of the mixture at the excitation wavelength is dominated by the ZnTPP Soret band (ca. 90%) and the transient absorption of C_{60} excited at this wavelength is considerably smaller than that of ZnTPP, the subtracted spectra are dominated by differences due to the latter. These differences are small, but reproducible and significant.

The considerable reduction of amplitude below 500 nm and the two relatively long-lived bands centered at 525 and 569 nm are immediately obvious. Scans over a longer time delay range (up to 900 ps) show almost no decay in these features indicating a lifetime $\gg 1$ ns, i.e., much longer than the lifetimes of the S_1 states of both ZnTPP and C_{60} .

Further, an extremely short-lived component centered at 650 nm can be observed. The kinetic trace at this wavelength shown in Figure 5E shows the rapid decay of this feature to the level of the overlapping, much longer-lived band ranging from 550 to 700 nm. Measurement of the rate of this decay is instrument-limited, but must be considerably faster than the ps rate of decay of the S_2 state of ZnTPP itself. It is therefore consistent with the rate requirements of the quenching process revealed by the steady state ZnTPP S_2 fluorescence quenching experiments.

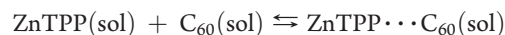
The transient absorption spectra of ZnTPP in benzonitrile in Figure 5F are again dominated by strong S_1 absorption bands around 537, 582, and 623 nm and the weaker short-lived S_2 absorption with a maximum near 660 nm. The transient spectrum of C_{60} in benzonitrile in Figure 5G shows a broad absorption with a minor maximum around 555 nm. A spectrally broader and much shorter-lived component with a maximum contribution near 563 nm is also observed.

As with the measurements in toluene, the ZnTPP + C_{60} mixture transient spectra recorded in benzonitrile shown in Figure 5H mostly resemble those of ZnTPP. However, the relative absorbance corrected subtracted spectra, 5I, clearly show key differences. There is evidence of long-lived species not decaying within the temporal excitation pulse separation of the experiment (10.6 μ s), despite measuring in aerated solution. The spectral features recorded prior to experimental time zero match those recorded at any point beyond in all but total amplitude, indicating that the prominent bands at the blue edge of the detection range, 534, 580, and 619 nm, are due to an extremely long-lived species. On the time scale of this measurement these features remain essentially constant in shape and amplitude. Again, a very short-lived component spectrally ranging from 600 to

680 nm, although much less obvious than in the toluene mixture spectrum, is discernible (cf. the kinetic trace in Supporting Information, Figure S5).

DISCUSSION

The optical spectra of Figure 1 are completely consistent with previous reports of the solution phase UV–visible absorption spectra of porphyrin–fullerene mixtures and supramolecular constructs, and provide no clear evidence of binding between ground state C_{60} and ZnTPP.¹⁷ Such an absence of effect of added fullerene on the optical absorption spectra might suggest that the ground state association constant, K_A , for the process:



is unusually small. However, high quality DFT calculations²² suggest that the binding energy between bare ZnTPP and C_{60} is significant—of the order of 0.5 eV. In addition, the mutual upfield ring current shifts that are observed in the NMR spectra of porphyrin–fullerene mixtures in arene solutions confirm that significant short-range heteromolecular solute–solute interactions do occur.¹⁷ Quantitatively, experimental chromatographic measurements show that the net enthalpy change associated with forming associated ZnTPP \cdots C_{60} pairs in toluene solution is ca. -6 kJ mol⁻¹, a relatively small value that is indicative of the enthalpic cost of displacing the arene solvent from both the porphyrin and the fullerene.^{1a,23} Given that net entropic effects are small, a value of $K_A = 3 \times 10^4$ M⁻¹ is then obtained for an entirely enthalpically driven association,²⁴ which is similar to the values of K_A found for many ZnTPP–ligand interactions. We conclude that the net binding energy between C_{60} and ZnTPP in toluene in the ground state is likely similar to that observed in other systems exhibiting π -stacking interactions, and consequently should result in an association constant of the order of 10^3 – 10^5 M⁻¹ at room temperature.

A net 6 kJ mol⁻¹ stabilization of the ground state of the ZnTPP chromophore by C_{60} in the present experiments would result in an easily measurable displacement of the ZnTPP UV–visible absorption bands if the excited state were not similarly affected. The fact that no significant shift is seen in the optical spectra with added fullerene therefore indicates that the binding energies of ZnTPP to C_{60} are almost the same in the ground and the electronically excited states, and that the absorption spectra of the uncomplexed and complexed ZnTPP overlap almost perfectly. Importantly, the fact that no significant change is observed in the intensities of the spectra in either the porphyrin Soret or Q-band regions with large excesses of added C_{60} suggests that the absorption bands of the ZnTPP \cdots C_{60} complexes have almost the same molar absorptivities as those of the uncomplexed porphyrin itself. Thus excitation of these ZnTPP + C_{60} solutions at any wavelength within either the Soret or Q-band regions will result in populating the excited states of the complexed and uncomplexed ZnTPP concurrently via transitions with the about same oscillator strength. This behavior of the ZnTPP + C_{60} system is therefore unlike those in which fullerenes substituted with potential dative ligands undergo self-assembly with a porphyrin via axial noncovalent binding.^{2,4,25} Such substituted fullerene–porphyrin pairings in solution exhibit distinct new red-shifted absorption bands with clear isosbestic points due to ground state complex formation and are characterized by values of K_A that are often $\gg 10^3$ M⁻¹.

The mechanism by which the electronically excited moiety relaxes in porphyrin–fullerene systems is of critical importance

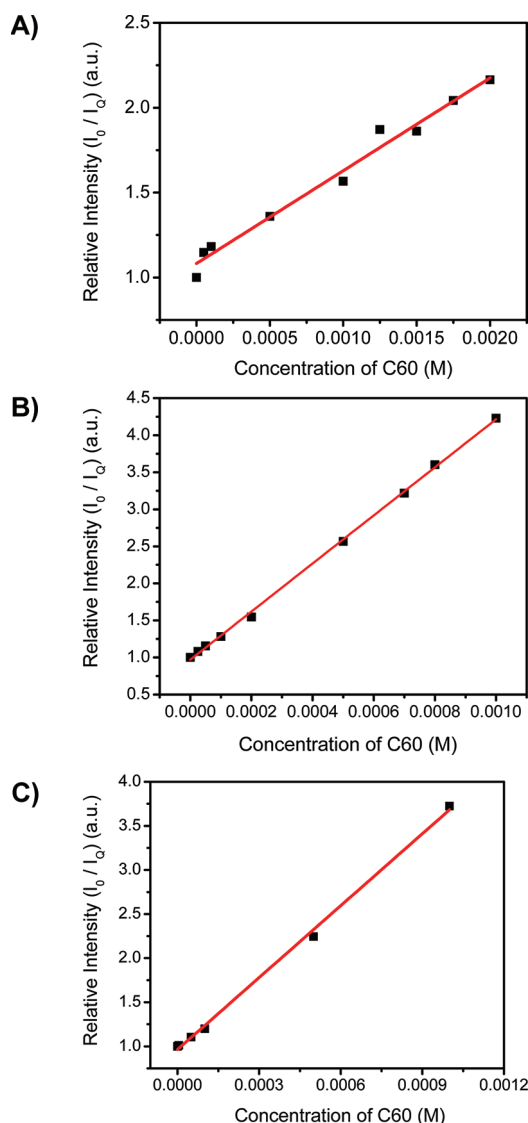


Figure 6. (A) Stern–Volmer plot derived from Figure 2A. Excitation at 550 nm and emission monitored at 655 nm. Slope = $(0.55 \pm 0.03) \times 10^3 \text{ M}^{-1}$. (B) Stern–Volmer plot derived from Figure 2B. Excitation at 400 nm and emission monitored at 432 nm. Slope = $(3.24 \pm 0.04) \times 10^3 \text{ M}^{-1}$. (C) Stern–Volmer plot derived from Figure S2, Supporting Information. Excitation at 407 nm and emission monitored at 655 nm. Slope = $(2.72 \pm 0.06) \times 10^3 \text{ M}^{-1}$.

in the design of photon-actuated devices. Considerations of excited state energies, spectral overlaps and redox parameters indicate that both energy transfer and electron transfer are possible for many electronically excited porphyrin–fullerene systems including the self-aggregating ZnTPP– C_{60} system studied here. Efficient long-range, Förster-type dipole–dipole energy transfer can easily be ruled out on the basis of small spectral overlaps and low oscillator strengths in the relevant C_{60} electronic transitions. However, in untethered 1:1 complexes in solution and in solid state aggregates in which the porphyrin and fullerene are at van der Waals separations, either short-range electron transfer or Dexter-type energy transfer are not only feasible, but also could occur at rates that are potentially competitive with radiationless decay of the local excited state produced on excitation in the porphyrin Soret band.

To elucidate the mode of excited state relaxation of the ZnTPP $\cdots \text{C}_{60}$ system examined here, Stern–Volmer type plots (Figure 6A–C) were constructed from the corrected steady state fluorescence quenching data presented in Figure 2A,B, respectively. Figure 6C presents data similar to that of Figure 6B, except that Q-band fluorescence was monitored when exciting in the Soret band. Surprisingly, all three Stern–Volmer plots are linear over the $0 < [\text{C}_{60}] \leq 10^{-3} \text{ M}$ concentration range employed (i.e., up to at least a 1000:1 molar ratio of C_{60} :ZnTPP).

ZnTPP S_1 fluorescence quenching by C_{60} could, in principle, take place by one or both of the well-known static and dynamic groups of mechanisms.²⁶ The lifetime of the ZnTPP S_1 state, τ_{S_1} , is close to 2.0 ns in fluid solution,²⁰ so the average $\text{C}_{60} \cdots \text{ZnTPP}$ diffusional displacement during this N/e population decay time will be given approximately by $\langle x \rangle = (2D\tau_{\text{S}_1})^{1/2} = 2 \text{ nm}$, using $D = 1 \times 10^{-9} \text{ m}^2 \text{ s}^{-1}$ for ZnTPP + C_{60} in toluene at room temperature.²⁷ A 2 nm displacement is considerably greater than the center-to-center ZnTPP to fullerene distances, which range from 0.29 to 0.35 nm in cocrystallized zinc metalloporphyrin $\cdots \text{C}_{60}$ and C_{70} aggregates in which van der Waals interactions dominate.²⁸ Because these data suggest that significant donor–acceptor diffusional displacement could occur in solution during the lifetime of the S_1 excited metalloporphyrin, analysis of the steady state quenching data of Figure 2A using a mixed static plus dynamic treatment would seem to be in order.

On the other hand, the lack of effect on the measured S_1 fluorescence lifetimes when large molar excesses of C_{60} are added to the ZnTPP solution (and the steady state fluorescence yields greatly diminished) suggests that we are observing almost exclusively Q-band excited ZnTPP that is not complexed in the ground state. Furthermore, the species that is produced following Q-band excitation of the complex must be almost completely dark and must be formed very rapidly (relative to the ns lifetime of an unperturbed S_1 excited state of ZnTPP) at a fixed ZnTPP $\cdots \text{C}_{60}$ distance. An extremely feeble, short-lived emission component that constitutes only 2% of the total emission at a C_{60} :ZnTPP ratio of 1000:1 can be observed in the ns time-resolved S_1 fluorescence decays. Apart from this, the only signal seen in the Q-band region is emission from the uncomplexed porphyrin, which of necessity is excited at the same wavelength and with the same oscillator strength as that of the complex.

The linear Stern–Volmer plot of Figure 6A is therefore interpreted as follows. A mixed static–dynamic quenching mechanism²⁶ yields the expression:

$$\frac{I_0}{I_Q} = (1 + K_D[\text{Q}])(1 + K_S[\text{Q}]) \quad (1)$$

where I_0 is the unquenched S_1 fluorescence intensity, I_Q is the reduced intensity at molar concentrations of C_{60} represented by $[\text{Q}]$ and K_D and K_S are the dynamic and static quenching constants in units of M^{-1} respectively. If K_D and K_S are of similar magnitude then eq 1 is quadratic in $[\text{Q}]$ and a curved Stern–Volmer plot is expected. Here, however, the reasonably linear plot shown in Figure 6A, and the above analysis suggest that $K_S \gg K_D$, so that (1) reduces to

$$\frac{I_0}{I_Q} = 1 + K_S[\text{Q}] \quad (2)$$

where K_S becomes identified with the measured Stern–Volmer constant, K_{SV} , which for S_1 “quenching” has a value of $K_{\text{SVS}_1} = (5.5 \pm 0.3) \times 10^2 \text{ M}^{-1}$. If K_D were much larger than K_S then K_D would be identified with $K_{\text{SV}} = k_{\text{Q}}\tau^0$. However, such an assumption produces a

value of $k_Q = K_D/\tau^0 = 2.8 \times 10^{11} \text{ M}^{-1} \text{ s}^{-1}$, which is a factor of at least 15 larger than the diffusion limited value²⁹ for a bimolecular dynamic quenching constant in toluene at room temperature. Thus $K_{\text{SVS1}} \approx K_S$, which, in turn, is usually identified with the association constant for the aggregation of ZnTPP with C_{60} in the ground state, i.e.

$$K_A = [\text{ZnTPP} \cdots C_{60}] / ([\text{ZnTPP}][C_{60}]) = (5.5 \pm 0.3) \times 10^2 \text{ M}^{-1}$$

For the S_2 state, the average excited chromophore-quencher diffusional displacement during the S_2 lifetime is $\langle x \rangle = (2D\tau_{S2})^{1/2} = 0.06 \text{ nm}$, using $D = 1 \times 10^{-9} \text{ m}^2 \text{ s}^{-1}$ for ZnTPP + C_{60} in toluene at room temperature and $\tau_{S2} = 1.4 \times 10^{-12} \text{ s}$. This value of $\langle x \rangle$ is much smaller than the average van der Waals spacing in this system, and a purely static quenching process (in the sense that the donor and acceptor will be essentially stationary during the lifetime of the porphyrin excited state) should therefore dominate the S_2 ZnTPP $\cdots C_{60}$ interaction. The observation that the ZnTPP S_2 fluorescence lifetime remains unchanged at 1.4 ps at all concentrations of C_{60} , including those at which the C_{60} :ZnTPP ratio is very large, suggests that, once again, only the emission from uncomplexed Soret-excited ZnTPP is being observed in these experiments. The conclusion must then be that the state produced following Soret band excitation of the ZnTPP $\cdots C_{60}$ complex is also dark and that the locally excited ZnTPP S_2 state is being quenched at a rate that is very fast compared with the inverse lifetime of the uncomplexed species, i.e., at a rate $\gg 10^{12} \text{ s}^{-1}$.

Note, however, that the value of the Stern–Volmer constant for C_{60} quenching of the S_2 emission of ZnTPP, $K_{\text{SVS2}} = 3.24 \times 10^3 \text{ M}^{-1}$, is a factor of about 6 larger than that for quenching the S_1 fluorescence under otherwise identical conditions. Therefore it is not a simple matter of ascribing the behavior of both excited porphyrin states to excitation of the ground state ZnTPP $\cdots C_{60}$; otherwise the same value of K_{SV} would result (i.e., K_{SVS1} should equal K_{SVS2} , which it is not). Because quenching must occur in the S_1 -excited complex on a time scale that is very fast compared with the rate of diffusional separation of C_{60} from ZnTPP, the smaller value of K_{SV} obtained for quenching of the S_1 -excited species cannot be ascribed to an averaging of quenching rates over an increasing range of C_{60} –ZnTPP spacings.

Let us assume for initial argument's sake that the mechanism of quenching involves short-range Dexter energy transfer to C_{60} when the ZnTPP $\cdots C_{60}$ complex is excited in both the Soret and Q bands of the porphyrin. In essence, excitation of the ground state complex instantaneously creates a weakly bound exciplex¹⁰ of the same geometry. The greater net rate of fluorescence quenching when the exciplex is in its S_2 state would then be ascribed to greater donor–acceptor wave function overlap. Is this reasonable?

The S_1 and S_2 states of ZnTPP are largely built from the same set of four molecular orbitals; the near-degenerate HOMO and HOMO–1 (a_{2u} and a_{1u} in D_{4h}) and the strictly doubly degenerate LUMO (e_g in D_{4h}). A TD-DFT description^{15b} reveals that the a_{2u} – e_g plus a_{1u} – e_g one-electron promotions contribute >95% and >85% respectively of the oscillator strengths of the S_1 – S_0 and S_2 – S_0 optical transitions. Thus the nominal spatial extent of the wave functions of ZnTPP in its S_1 and S_2 states will be very similar. However, the linear decrease in the S_2 – S_1 electronic energy gap of ZnTPP and other metalloporphyrins with increasing solvent Lorenz–Lorentz polarizability function demonstrates^{3b,c} that the polarizability of the molecule is significantly greater in the S_2 state than in S_1 . Thus a slightly greater excited donor–acceptor wave function overlap would be expected when the ZnTPP $\cdots C_{60}$

complex is excited in the Soret band compared with the Q-band, qualitatively consistent with an increased rate of energy transfer by the Dexter mechanism. On the other hand, even when the C_{60} :ZnTPP molar ratio is very large there is no evidence of increased emission (relative to C_{60} alone) in the 13000 cm^{-1} to 16000 cm^{-1} region in either toluene or benzonitrile where electronically excited singlet C_{60} has been reported²⁹ to emit. The emission spectra thus provide no direct evidence of either direct energy transfer to C_{60} or the population of electronically excited C_{60} via charge recombination in an intermediate charge-separated species.³⁰ We note however, that this may not be a definitive indicator of the absence of electronically excited C_{60} because (i) its fluorescence quantum yield in this region³⁰ is of the order of 10^{-4} and (ii) only a small fraction of the C_{60} in solution is complexed and capable of acting as an energy acceptor following excitation in the porphyrin Soret band.

The alternative quenching mechanism involves short-range electron transfer in the ZnTPP $\cdots C_{60}$ exciplex. A multitude of previous studies^{10,31} have shown that the driving force for electron transfer from excited ZnTPP (donor) to ground state C_{60} (acceptor) is favorable when the porphyrin is excited to both the S_1 and S_2 states, i.e., $\Delta G_{\text{ET}} < 0$ in both cases. Irrespective of the uncertainties associated with the measurement of redox potentials and solvent stabilization energies using the Rehm–Weller approach,³² here we can be sure that the difference in driving force for electron transfer in the two electronic states of ZnTPP will be precisely equal to their energy spacing in the solvent in question. That is, $\Delta G_{\text{ET},S2} - \Delta G_{\text{ET},S1} = \Delta \Delta G_{\text{ET}} = -\Delta E(S_2 - S_0) = -0.81 \text{ eV}$ for ZnTPP in toluene, provided that the radical anion and cation are produced in the same electronic state in both cases. Using a reasonable set of redox potentials for ZnTPP and C_{60} in the nonpolar solvent toluene (for which the solvent stabilization energy is C) yields $-\Delta G_{\text{ET},S2} = (1.3 + C) \text{ eV}$ and $-\Delta G_{\text{ET},S1} = (0.5 + C) \text{ eV}$ when $C_{60}^{\bullet-}$ is produced in its ground state. In polar solvents, C is approximately 0 but may be as large as 1 eV in nonpolar solvents such as toluene.³² However, for at least the Soret-excited systems such as these where both complexed molecules are rigid and all competing intermolecular processes must occur on a subps time scale, it can be reasonably argued^{3e} that C approaches zero even in nonpolar solvents.

For a covalently bound ZnTPP– C_{60} dyad in a nonpolar solvent¹⁰ these data would normally place the S_1 electron transfer rate near the maximum of the Marcus parabola and that for S_2 in the inverted region. On this basis alone one might predict a smaller electron transfer rate from S_2 compared with S_1 , contrary to the observed faster rate of S_2 fluorescence quenching. However, inasmuch as a variety of electronically excited states are likely available to the product radical ions, we cannot be sure that the ground state(s) is the initial product state. For example, if $C_{60}^{\bullet-}$ were produced in its lowest electronically excited doublet state, ΔG_{ET} would be reduced in magnitude by the electronic excitation energy of the radical anion, 1.55 eV for the uncomplexed species in CH_2Cl_2 /toluene.³³ Thus, it could be that the rate of electron transfer in the Q-band excited complex would fall in the normal Marcus region whereas that of the Soret-band excited species, falling near the barrierless region, would be faster. A similar situation has recently been described by Hammarström, et al.³⁴ in which forward electron transfer in a Soret-excited, water-soluble zinc porphyrin–viologen complex produces an electronically excited charge transfer state.

In principle, ps transient absorption spectra such as those in Figure 5A–I should provide evidence to distinguish between the electron and energy transfer mechanisms. The identification of

transient species formed on the ps time scale of the ZnTPP S_2 state is the key to this; electron transfer from the Soret-excited ZnTPP to C_{60} would yield the $ZnTPP^{+•} + C_{60}^{•-}$ radical ion pair. The absorption spectra of the ZnTPP radical cation,³⁵ $ZnTPP^{+•}$, and the C_{60} radical anion,³³ $C_{60}^{•-}$ are well-known both as individual species and as ion pairs, and are clearly seen in ns transient absorption spectra^{1b,11} following charge transfer from the lowest triplet state of ZnTPP to C_{60} . The observation of the ground state of $C_{60}^{•-}$ in the near-infrared was beyond the spectral detection range of the transient absorption detection system. Therefore the identification of the porphyrin radical cation was the only means of testing this hypothesis in these experiments. The presence of several absorbing species within the ZnTPP + C_{60} mixture, i.e., both unbound and complexed components, is a serious complication due to overlapping contributions to the transient spectra. Therefore the difference spectra shown in Figure 5D,I, together with the corresponding kinetic traces, provide the most useful information. Due to the higher solubility and therefore higher concentration of C_{60} employed in the toluene measurements, the ratio of complexed to free ZnTPP will be significantly greater in toluene than in benzonitrile. Consequently the difference spectra in toluene contain a better signal-to-noise ratio.

On the longer time scales of the measurements in toluene the difference spectrum shows both the lowered concentration of a species absorbing in the 460 nm region and an increased concentration of a species absorbing in the region above 530 nm, which, considering their very similar yet inverted time profiles, suggests a reactant-product relationship. One possible interpretation is that the ZnTPP S_1 state, which is rapidly formed via internal conversion from the initially excited S_2 state in the complex, undergoes electron transfer to C_{60} on a ps time-scale, therefore lowering the S_1 and increasing the radical cation contributions in the mixture. The additional, much shorter-lived component centered around 650 nm both forms more rapidly than the features assigned to the ZnTPP S_1 state and decays more rapidly than the unquenched S_2 state lifetime. The 650 nm feature could be the product of electron transfer from the S_2 state to C_{60} in the complexed species to form an electronically excited charge separated state with a slightly spectrally shifted and more intense molar absorptivity compared to the lowest energy charge separated state. The more rapid decay of this feature compared with the charge separated state originating from S_1 suggests that it may relax by charge recombination to a vibrationally excited ground state.

The presence of an extremely long-lived species in the benzonitrile ZnTPP + C_{60} mixture measurements is consistent with the stabilization of charge separated states by a polar solvent. No such feature is seen in the single-solute ZnTPP or C_{60} measurements in benzonitrile, further confirming this interpretation. Considerations of diffusion rates (vide supra) complicate the attribution of this transient to excitation of a ground state complex or to collisions during the relatively long ZnTPP T_1 state lifetime. The very short-lived component centered around 660 nm, however, suggests an interpretation similar to that found in the toluene mixtures, i.e., fast electron transfer from the S_2 state to an excited charge separated state followed by rapid charge recombination to a vibrationally excited ZnTPP ground state. The lower relative intensity of this feature can be attributed to the smaller fraction of complexes in these solutions due to the lower concentration of C_{60} employed in this solvent.

These transient absorption measurements do not quantify the amounts of the various species observed; we cannot rule out

parallel energy and electron transfer relaxation processes. Nevertheless, these experiments do provide, for the first time, qualitative spectroscopic evidence for the formation of charge-transfer species on a subps time scale when noncovalently bound, self-assembled porphyrin–fullerene complexes are initially excited in the Soret band. The ion pairs formed by charge transfer eventually relax to the ground states of their components. Curiously, qualitative support for this overall mechanism may be found in measurements of the extent of photodegradation of the ZnTPP during the transient absorption experiments. When alone in the aerated toluene and benzonitrile solvents, ZnTPP degrades significantly more than when the same concentration of ZnTPP in the same aerated solvent containing a large excess of C_{60} is subjected to the same total radiant exposure. That is, the C_{60} acts as a photoprotective agent in these experiments.

Finally, we note that the novel features in the ps transient absorption spectra of uncomplexed ZnTPP that relax with the same time constants as S_2 fluorescence in fluorescence upconversion experiments must be assigned to absorptions of the S_2 state of the metalloporphyrin itself. Assuming that the origin of this absorption lies near 650 nm we predict that the origin of a higher gerade singlet state of ZnTPP must be located near 4.8 eV (255 nm), and is accessed from the S_2 (2^1E_u) state by an allowed one-photon transition having substantial oscillator strength. Time-dependent density functional theory calculations^{15b} reveal several gerade singlet electronic states lying above the 2^1E_u state of ZnTPP, but these calculations do not extend to states above 3.5 eV. Two-photon absorption cross sections of ZnTPP, which would reveal g–g electronic spacings, have not been measured in the needed spectral region.

CONCLUSIONS

Although many spectroscopic and photophysical studies of Soret-excited, porphyrin–fullerene supramolecular constructs have been undertaken, the work reported herein provides the first published information on the photophysical behavior of the model, noncovalently self-assembled, Soret-excited ZnTPP + C_{60} system in fluid solution. Despite the unavoidable complication of simultaneous excitation of uncomplexed and complexed ZnTPP in these experiments, clear evidence of ultrafast quenching of the locally S_2 -excited state of ZnTPP in the ZnTPP $\cdots C_{60}$ complex has been obtained from both steady state and ps transient absorption measurements.

Two possible quenching mechanisms, short-range electronic energy transfer and electron transfer in the excited complex, have been evaluated. The first direct evidence of the formation, on a subps time scale, of long-lived, charge-separated transients has been obtained for these Soret-excited complexes. Although the existence of parallel energy and electron transfer relaxation processes cannot be ruled out, relaxation processes bypassing the locally excited S_1 state have been revealed. The lower excited state of the complex is not populated quantitatively following Soret excitation.

These results may prove to be of considerable importance in the future design of photonic devices, sensors and organic solar cells that make use of direct excitation or photon upconversion to the higher electronic states of the metalloporphyrins.

ASSOCIATED CONTENT

S Supporting Information. (i) Description of the corrections to the ZnTPP fluorescence intensities due to competitive

absorption by C₆₀. (ii) Changes in the absorbance of the Soret and Q-bands of ZnTPP with added C₆₀. (iii) ZnTPP S₁ fluorescence spectra obtained by exciting at 400 nm in the Soret band, with quenching by C₆₀. Comparison of the S₁ fluorescence spectra of ZnTPP with a large excess of C₆₀ when excited at 550 and 400 nm. (iv) S₁ fluorescence decay data obtained by time-correlated single photon counting for Soret-excited ZnTPP with a large excess of C₆₀ in toluene. (v) Picosecond S₁ fluorescence rise profiles obtained by exciting ZnTPP at 400 nm, with added C₆₀. (vi) Kinetics of the formation on a picosecond time scale of a long-lived transient in the ZnTPP + C₆₀ system in benzonitrile. This material is available free of charge via the Internet at <http://pubs.acs.org>.

AUTHOR INFORMATION

Corresponding Author

*E-mail: K.P.G., ghiggino@unimelb.edu.au; M.F.P., matthew.paige@usask.ca; R.P.S., ron.steer@usask.ca.

Note

⁵On leave from Faculty of Applied Physics and Mathematics, Gdańsk University of Technology, Gdańsk, Poland.

ACKNOWLEDGMENT

Acknowledgment is made to the donors of the American Chemical Society Petroleum Research Fund for support of this research. The authors gratefully acknowledge the ongoing support by the Natural Sciences and Engineering Research Council of Canada for operations and by the Canada Foundation for Innovation and the Province of Saskatchewan for infrastructure. KPG thanks the Australian research Council for financial support. Assistance of Mr. Brook Danger with TCSPC experiments and laser technical training by Dr. Sophie Brunet are gratefully acknowledged.

REFERENCES

- (1) For recent reviews relevant to this paper see: (a) Orlandi, G.; Negri, F. *Photochem. Photobiol. Sci.* **2002**, *1*, 289–308. (b) El-Khouly, M. E.; Ito, O.; Smith, P. M.; D'Souza, F. D. *J. Photochem. Photobiol. C* **2004**, *5*, 79–104. (c) Boyd, P. D. W.; Reed, C. A. *Acc. Chem. Res.* **2005**, *38*, 235–242. (d) D'Souza, F. D.; Ito, O. *Coord. Chem. Rev.* **2005**, *249*, 1410–1422. (e) Thomas, K. G.; George, M. V.; Kamat, P. V. *Helv. Chim. Acta* **2005**, *88*, 1291–1308. (f) Tashiro, K.; Aida, T. *Chem. Soc. Rev.* **2007**, *36*, 189–197. (g) Drain, C. M.; Varotto, A.; Radivojevic, I. *Chem. Rev.* **2009**, *109*, 1630–1658. (h) Beletskaya, I.; Tyurin, V. S.; Tsivadze, A. U.; Guillard, R.; Stern, C. *Chem. Rev.* **2009**, *109*, 1659–1713. (i) Accorsi, G.; Armaroli, N. *J. Phys. Chem. C* **2010**, *114*, 1385–1403. (j) Grimm, B.; Hausmann, A.; Khant, A.; Seitz, W.; Spänig, F.; Guldi, D. M. in *Handbook of Porphyrin Science*, Vol. 1, Supramolecular Chemistry, K.M. Kadish, K. M.; Smith, K. M.; Guillard, R., Eds. World Scientific, Singapore, 2010, p133. (k) D'Souza, F.; Ito, O. *ibid.*, p. 307.
- (2) (a) Bell, T. D. M.; Ghiggino, K. P.; Jolliffe, K. A.; Ranasinghe, M. G.; Langford, S. J.; Shephard, M. J.; Paddon-Row, M. N. *J. Phys. Chem. A* **2002**, *106*, 10079–10088. (b) Milanese, M. E.; Gervald, M.; Otero, L. A.; Sereno, L.; Silber, J. J.; Durantini, E. N. *J. Phys. Org. Chem.* **2002**, *15*, 844–851. (c) Vail, S. A.; Tomé, J. P. C.; Krawczuk, P. J.; Dourandin, A.; Shafirovitch, V.; Cavaleiro, J. A. S.; Schuster, D. A. *J. Phys. Org. Chem.* **2004**, *17*, 814–818. (d) Imahori, H. *Org. Biomol. Chem.* **2004**, *2*, 1425–1433. (e) Nierengarten, J. F. *New J. Chem.* **2004**, *28*, 1177–1191. (f) Gunes, S.; Neugebauer, H.; Sariciftci, N. S. *Chem. Rev.* **2007**, *107*, 1324–1338. (g) Imahori, H.; Umeyama, T. *J. Phys. Chem. C* **2009**, *113*, 9029–9039. (h) Megiatto, J. D.; Schuster, D. I.; Abwander, S.; de Miguel, G.; Guldi, D. M. *J. Am. Chem. Soc.* **2010**, *132*, 3847–3861. (i) Pal, S. K.; Kesti, T.; Maiti, M.; Zhang, F.; Inganaas, O.; Hellstroem, S.; Andersson, M. R.; Oswald, F.; Langa, F.; Oesterman, T.; Pascher, T.; Arkady, Y.; Sundström, V. *J. Am. Chem. Soc.* **2010**, *132*, 12440–12451.
- (3) (a) Steer, R. P. *J. Appl. Phys.* **2007**, *102*, 076102/1–076102/3. (b) Tripathy, U.; Liu, X.; Kowalska, D.; Velate, S.; Steer, R. P. *J. Phys. Chem. A* **2008**, *112*, 5824–5833. (c) Liu, X.; Tripathy, U.; Bhosale, S. V.; Langford, S. J.; Steer, R. P. *J. Phys. Chem. A* **2008**, *112*, 8986–8998. (d) Sugunan, S. K.; Tripathy, U.; Brunet, S. M.; Paige, M. F.; Steer, R. P. *J. Phys. Chem. A* **2009**, *113*, 8548–8556. (e) Maiti, M.; Danger, B. R.; Steer, R. P. *J. Phys. Chem. A* **2009**, *113*, 11318–11326. (f) O'Brien, J. A.; Rallabandi, S.; Tripathy, U.; Paige, M. F.; Steer, R. P. *Chem. Phys. Lett.* **2009**, *475*, 220–222.
- (4) Danger, B. R.; Bedient, K.; Maiti, M.; Burgess, I. J.; Steer, R. P. *J. Phys. Chem. A* **2010**, *114*, 10960–10968.
- (5) Szmytkowski, J.; Bond, T.; Paige, M. F.; Scott, R. W. J.; Steer, R. P. *J. Phys. Chem. A* **2010**, *114*, 11471–11476.
- (6) (a) Balushev, S.; Miteva, T.; Yakutin, V.; Nelles, G.; Yasuda, A.; Wegner, G. *Phys. Rev. Lett.* **2006**, *97*, 143903/1–143903/3. (b) Balushev, S.; Yakutin, V.; Wegner, G.; Minch, B.; Miteva, T.; Nelles, G.; Yasuda, A. *J. Appl. Phys.* **2007**, *101*, 023101/1–023101/2. (c) Cheng, Y. Y.; Khoury, T.; Clady, R. G. C. R.; Tayabjee, M. J. Y.; Elkins-Dauks, N. J.; Crossley, M. J.; Schmidt, T. W. *Phys. Chem. Chem. Phys.* **2010**, *12*, 66–71. (d) Cheng, Y. Y.; Fückel, B.; Khoury, T.; Clady, R. G. C. R.; Tayabjee, M. J. Y.; Elkins-Dauks, N. J.; Crossley, M. J.; Schmidt, T. W. *J. Phys. Chem. Lett.* **2010**, *1*, 17951799. (e) Singh-Rachford, T. N.; Castellano, F. N. *Coord. Chem. Rev.* **2010**, *254*, 2560–2573 and references therein.
- (7) Tripathy, U.; Steer, R. P. *J. Porphyrins Phthalocyanines* **2007**, *11*, 228–243.
- (8) (a) Maciejewski, A.; Steer, R. P. *Chem. Rev.* **1993**, *93*, 67–98. (b) Eisenberger, H.; Nickel, B.; Ruth, A. A.; Steer, R. P. *J. Chem. Soc., Faraday Trans.* **1996**, *92*, 741–746.
- (9) (a) Nickel, B. *Helv. Chim. Acta* **1978**, *61*, 198–222. and references therein. (b) Burdzinski, G.; Kubicki, J.; Maciejewski, A.; Steer, R. P.; Velate, S.; Yeow, E. K. L. in *"Molecular and Supramolecular Photochemistry"*, Vol. 14, Ramamurthy, V.; Schantze, K. S.; Eds., Taylor and Francis, New York, 2005, 1.
- (10) (a) For a review see: Mataga, N.; Chosrowjan, H.; Taniguchi, S. *J. Photochem. Photobiol. C* **2005**, *6*, 37–79. (b) Mataga, N.; Chosrowjan, H.; Shibata, Y.; Yoshida, N.; Osuka, A.; Kikuzawa, T.; Okuda, I. *J. Am. Chem. Soc.* **2001**, *123*, 12422–12423. (c) Mataga, N.; Chosrowjan, H.; Taniguchi, S.; Shibata, Y.; Yoshida, N.; Osuka, A.; Kikuzawa, T.; Okada, T. *J. Phys. Chem. A* **2002**, *106*, 12191–12201. (d) Mataga, N.; Taniguchi, S.; Chosrowjan, H.; Osuka, A.; Yoshida, N. *Photochem. Photobiol. Sci.* **2003**, *2*, 493–500. (e) Mataga, N.; Taniguchi, S.; Chosrowjan, H.; Osuka, A.; Yoshida, N. *Chem. Phys.* **2003**, *295*, 215–228.
- (11) (a) Nojiri, T.; Watanabe, A.; Ito, O. *J. Phys. Chem. A* **1998**, *102*, 5215–5219. (b) El-Khouly, M. E.; Fujitsuka, M.; Ito, O. *J. Porphyrins Phthalocyanines* **2000**, *4*, 590–597.
- (12) Kesti, T.; Tkachenko, N.; Yamada, H.; Imahori, H.; Fukuzumi, S.; Lemmetyinen, H. *Photochem. Photobiol. Sci.* **2003**, *2*, 251–258.
- (13) (a) Kesti, T. J.; Tkachenko, N. V.; Vehmanen, V.; Yamada, H.; Imahori, H.; Fukuzumi, S.; Lemmetyinen, H. *J. Am. Chem. Soc.* **2002**, *124*, 8067–8077. (b) Yamada, H.; Ohkubo, D.; Takahashi, T.; Sandanayaka, A. S. D.; Okujima, T.; Ohara, K.; Ito, O.; Uno, H.; Ono, N.; Fukuzumi, S. *J. Phys. Chem. B* **2010**, *114*, 14717–14728.
- (14) Gun'kin, I. F.; Loginova, N. Yu. *Russ. J. Gen. Chem.* **2006**, *76*, 1911–1913.
- (15) (a) Yeow, E. K. L.; Steer, R. P. *Phys. Chem. Chem. Phys.* **2003**, *5*, 97–105. (b) Liu, X.; Yeow, E. K. L.; Velate, S.; Steer, R. P. *Phys. Chem. Chem. Phys.* **2006**, *8*, 1298–1309.
- (16) Yao, C.; Kraatz, H.-B.; Steer, R. P. *Photochem. Photobiol. Sci.* **2005**, *4*, 191–199.
- (17) (a) Boyd, P. D. W.; Hodgson, M. C.; Rickard, C. E. F.; Oliver, A. G.; Chaker, I.; Brothers, P. J.; Bolskar, R. D.; Tham, F. S.; Reed, C. A. *J. Am. Chem. Soc.* **1999**, *121*, 10487–10495. (b) Wahadoszamen, M.; Nakabayashi, T.; Kang, S.; Imahori, H.; Ohta, N. *J. Phys. Chem. B* **2006**, *110*, 20354–20361.

- (18) (a) Litvinov, A. L.; Konarev, D. V.; Kovalevsky, A. Y.; Neretin, I. S.; Coppens, P.; Lyubovskaya, R. N. *Cryst. Growth Des.* **2005**, *5*, 1807–1819. (b) Zakharova, I. B.; Donenko, E. A.; Biryulin, Y. F.; Sharonova, L. V.; Makarova, T. L. *Fullerenes Nanotubes and Carbon Nanostructures* **2008**, *16*, 424–429.
- (19) Bhattacharya, S.; Ujihashi, N.; Aonuma, S.; Kimura, T.; Komatsu, N. *Spectrochim. Acta A* **2007**, *68*, 495–503.
- (20) Kowalska, D.; Steer, R. P. *J. Photochem. Photobiol. A* **2008**, *195*, 223–227.
- (21) (a) Yu, H.-Z.; Baskin, J. S.; Zewail, A. H. *J. Phys. Chem. A* **2002**, *106*, 9845–9854. (b) Lukaszewicz, A.; Karolczak, J.; Kowalska, D.; Maciejewski, A.; Ziolk, M.; Steer, R. P. *Chem. Phys.* **2007**, *331*, 359–372.
- (22) (a) Liao, M.-S.; Watts, J. D.; Huang, M.-J. *J. Phys. Chem. B* **2007**, *111*, 4374–4382. (b) Liao, M.-S.; Watts, J. D.; Huang, M.-J. *Phys. Chem. Chem. Phys.* **2009**, *11*, 4365–4374.
- (23) J. Xiao, J.; Meyerhoff, M. E. *J. Chromatog. A* **1995**, *715*, 19–29.
- (24) Hosseini, A.; Taylor, S.; Accorsi, G.; Armaroli, N.; Reed, C. A.; Boyd, P. D. W. *J. Am. Chem. Soc.* **2006**, *128*, 15903–15913.
- (25) Flamigni, L.; Ventura, B.; Oliva, A. I.; Ballester, P. *Chem.—Eur. J.* **2008**, *14*, 4214–4224.
- (26) Lakowicz, J. R., *Principles of Fluorescence Spectroscopy*, Springer, New York, 2006.
- (27) Saiki, H.; Takami, K.; Tominaga, T. *Phys. Chem. Chem. Phys.* **1998**, *1*, 303–306.
- (28) Konarev, D. V.; Kovalevsky, A.; Yu., Li, X.; Neretin, I. S.; Litvinov, A. L.; Drichko, N. V.; Slovokhotov, Y. L.; Coppens, P.; Lyubovskaya, R. N. *Inorg. Chem.* **2002**, *41*, 3638–3646.
- (29) Obtained using the Stokes–Einstein equation and a toluene solvent viscosity of 0.587 cP at 293K.
- (30) Accorsi, G.; Armaroli, N. *J. Phys. Chem. C* **2010**, *114*, 1385–1403.
- (31) Imahori, H.; El-Khouly, M. E.; Fujitsuka, M.; Ito, O.; Sakata, T.; Fukuzumi, S. *J. Phys. Chem. A* **2001**, *105*, 325–332 and references therein.
- (32) (a) Rehm, D.; Weller, A. *Ber. Bunsenges. Phys. Chem.* **1969**, *73*, 834–839. (b) Weller, A. *Z. Phys. Chem. N. F.* **1982**, *133*, 93–98.
- (33) Greaney, M. A.; Gorun, S. M. *J. Phys. Chem.* **1991**, *95*, 7142–7144.
- (34) (a) Andersson, M.; Davidsson, J.; Hammarström, L.; Korppi-Tommola, J.; Peltola, T. *J. Phys. Chem. B* **1999**, *103*, 3258–3262. (b) Petersson, J.; Eklund, M.; Davidsson, J.; Hammarström, L. *J. Phys. Chem. B* **2010**, *114*, 14329–14338.
- (35) Fajer, J.; Borg, D. C.; Forman, A.; Dolphin, D.; Felton, R. H. *J. Am. Chem. Soc.* **1970**, *92*, 3451–3459.